Density functional calculation of transition metal adatom adsorption on graphene

2008 J. Phys.: Condens. Matter 20 115209

(http://iopscience.iop.org/0953-8984/20/11/115209)

IOP PUBLISHING JOURNAL OF PHYSICS: CONDENSED MATTER

J. Phys.: Condens. Matter **20** (2008) 115209 (6pp) doi:10.1088/0953-8984/20/11/115209

Density functional calculation of transition metal adatom adsorption on graphene

Yuliang Mao[1,3], **Jianmei Yuan**[2] **and Jianxin Zhong**[1,3]

[1] Institute for Quantum Engineering and Micro-Nano Energy Technology, Xiangtan
University, Xiangtan 411105, Hunan,
People's Republic of China
[2] Hunan Key Laboratory for Computation and Simulation in Science and Engineering,
School of Mathematics and Computational Science in Xiangtan University, 411105, Hunan,
People's Republic of China

E-mail: ylmao@xtu.edu.cn and jxzhong@xtu.edu.cn

Received 16 September 2007, in final form 26 January 2008
Published 20 February 2008
Online at stacks.iop.org/JPhysCM/20/115209

Abstract

The functionalization of graphene (a single graphite layer) by the addition of transition metal atoms of Mn, Fe and Co to its surface has been investigated computationally using density functional theory. In the calculation, the graphene surface supercell was constructed from a single layer of graphite (0001) surface separated by vertical vacuum layers 2 nm thick. We found that the center of the hexagonal ring formed by carbon from graphene is the most stable site for Mn, Fe, Co to stay after optimization. The calculated spin-polarized band structures of the graphene encapsulating the Mn adatom indicate that the conduction bands are modified and move down due to the coupling between the Mn atom and graphene. For Fe adsorbed on the graphene surface, it is semi-half-metallic, and the spin polarization P is found to be 100%. The system of Co adatom on graphene exhibits metallic electronic structure due to the density of states (DOS) peak at the band center with both majority and minority spins. Local density of states analyses indicate a larger promotion of 4s electrons into the 3d state in Fe and Co, resulting in lower local moments compared to an Mn adatom on the graphite surface.

(Some figures in this article are in colour only in the electronic version)

Several experimental groups have successfully produced isolated, and room-temperature stable, two-dimensional (2D) crystals of graphene—a single layer of carbon atoms densely packed in a honeycomb crystal lattice [1–3]. For pure graphene, it is a semi-metal because, although there is a state crossing at the corner (K point) of the hexagonal Brillouin zone (BZ), the density of states there is zero [4]. The peculiar band structure in ultrathin graphite layers results in a number of unusual electronic transport properties, such as an anomalous quantum Hall effect [5, 6]. Because the linear band spectrum is a robust feature of the honeycomb lattice, the excitations in graphene are particles with zero effective mass that propagate coherently very large distances disregarding the amount of impurities, allowing graphene to sustain supercurrents [7]. By applying a bias voltage, the carrier density of graphene can be controlled by the electric field effect, allowing for many practical applications ranging from the production of electronic lenses [8] to the fabrication of semiconductors with a tunable gap in bilayers [9].

A number of theoretical studies have also been performed in order to provide an atomic-level understanding of the interactions between adatoms and graphene. These investigations focused on the stable configurations of metal adatoms on graphene [10], mixed hybridization in inducing magnetism [11, 12], and charge transfer between metal adatoms and graphene [13]. Using first-principles calculations, it was shown that the adsorption of atomic hydrogen on graphene opened a substantial gap in the electronic density of states, in which there lay a spin-polarized gap state [14]. Recent spin-polarized *ab initio* calculations have found that the carbon adatoms on graphene have a magnetic moment of about 0.5 μ_B [15].

One of the roads still unexplored in the materials science of graphene is the tailoring of its electronic properties by

---

[3] Authors to whom any correspondence should be addressed.

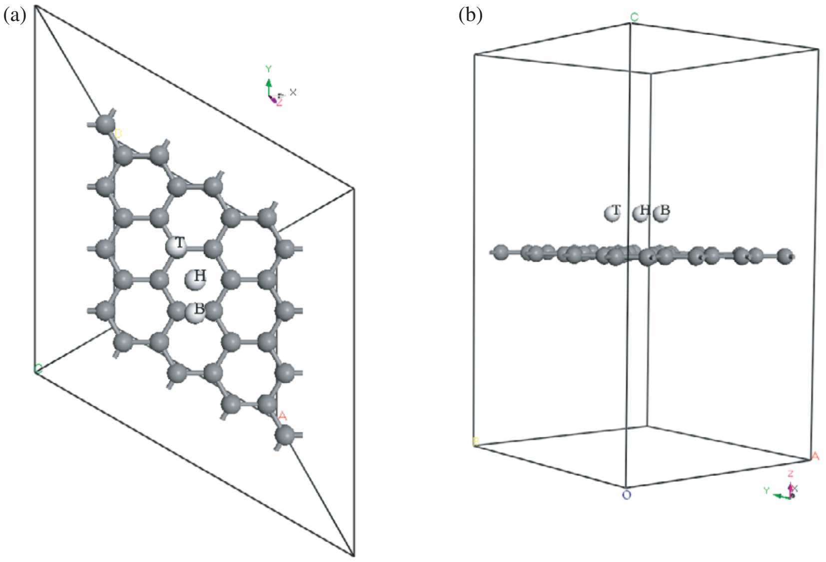

Figure 1. Typical configurations of the adatom–graphene system: (a) top view and (b) side view. H, B and T sites correspond to the positions where the adatom (white circle) is positioned above the center of a hexagonal ring formed by carbon atoms, above a C–C bond, and on top of a carbon atom, respectively.

chemical adsorption of transition metal (TM) atoms. The electronic properties that result from adsorption depend strongly on the ionic and covalent character of the bonds formed between carbon and the metal. Because of the strong electron–electron interactions in these materials, they are more susceptible to inducing a variation in the spin electronic structure. The tuning of the electronic structure in TM-coated graphene may open new routes for designing spintronics devices [16]. Therefore, it is interesting to investigate how its spin electronic structure changes by adsorbing TM adatoms on its surface. The atomic size of the TMs is an important factor in developing such nanostructures. From the relative sizes of C and the TMs, 3d elements such as Mn, Fe and Co are more suitable for doping, as the strain in the C–C bonds can be minimized. These TMs are also well suited for magnetism in such nanostructures. This paper is devoted to the numerical estimation of the bond lengths and magnetic moments for Mn, Fe, and Co atoms deposited on top of a flat graphene sheet. We also focus on studying the modulation of the spin electronic properties of graphene by adsorbing adatoms of Mn, Fe and Co. The estimate is performed by the density functional theory (DFT) method using CASTEP code. The largest magnetic moment, as well as the largest bond length, is found for Mn. The most symmetric position in the xy graphene plane (denoted H in figure 1) is the one which is energetically favorable for all atoms.

Our first-principles calculations were performed using spin-polarized DFT implemented in a CASTEP package [17], which is based on the plane-wave pseudopotential method. DFT is an extremely successful approach for the description of the ground-state properties of metals, semiconductors, and insulators. The main idea of DFT is to describe an interacting system of fermions via its density and not via its many-body wavefunction. This numerical technique, in spite of not explicitly accounting for the van der Waals part of the interlayer interaction, has been proved to give the correct equilibrium structure and to be accurate enough to tackle the complex band structure of three-dimensional (3D) graphite and carbon nanotubes in the vicinity of the Fermi energy (E_F) [18–22]. In our calculation, the generalized gradient approximation (GGA) proposed by Perdew, Burke, and Ernzerhof (PBE) [23] is used to deal with the exchange and correlation term. Ultrasoft pseudopotentials [24] and an energy cutoff of 600 eV, representing the number of plane-wave basis sets, are used. The Brillouin zone integration is performed within the Monkhorst–Pack scheme [25] using $4 \times 4 \times 2$ k points. The optimal atomic positions are determined until the magnitude of the forces acting on all atoms is less than 0.001 eV $Å^{-1}$ (which converges the total energy within 0.01 meV). Finite basis set corrections are also included.

In our calculation, the adatoms were first placed in high-symmetry positions (H, B and T sites) and then relaxed. The configurations of the adatom–graphene system are shown in figure 1. It is common for the ground-state structure found in such systems to distort from such high-symmetry positions, lowering the overall symmetry of the system. After the locally stable configurations have been found in the high-symmetry positions, the adatoms are displaced in a direction that fully breaks the symmetry of the system before re-relaxing. The calculated 4×4 supercell of the adatom–graphene system in figure 1 contains 32 carbon atoms and one TM adatom. The 4×4 supercell ensures a large distance of about 10 Å for the separation between neighboring adatoms in xy plane. It is necessary to ensure that the z-axis of the periodic supercell (perpendicular to the graphene layer) is large enough so that there is no interaction between graphene sheets of adjacent supercells. A distance of 20 Å along the z-axis was found to be sufficient to ensure energy convergence for configurations in figure 1. We note that, even though our purpose is to reveal the features of surface functionalization of mono- and bi-layer

Table 1. Summary of results for transition metal adatoms adsorbed on graphene. The adsorption energy is defined in the text. The values of the magnetic moment μ (μ_B) are for the local magnetic moments of the adatoms. The number of nearest carbon neighbors is indicated in parentheses following the value of the adatom–C bond length (Å). The height (Å) is the perpendicular distance from the adatom to the initial surface plane of graphene layer. The charge (e) transferred from the transition metal atom to the graphene is also indicated. The magnetic moment, bond length, height, and charge are for the most stable configurations (H site).

	Adsorption energy (eV)						
Adatom	H	B	T	Magnetic moment (μ_B)	Bond length (Å)	Height (Å)	Charge (e)
Mn	−0.93	−0.76	−0.76	5.62	2.52 (6)	2.05	0.84
Fe	−1.42	−0.68	−0.25	2.20	2.08 (6)	1.47	1.28
Co	−1.32	−0.66	−0.58	1.10	2.09 (6)	1.56	1.10

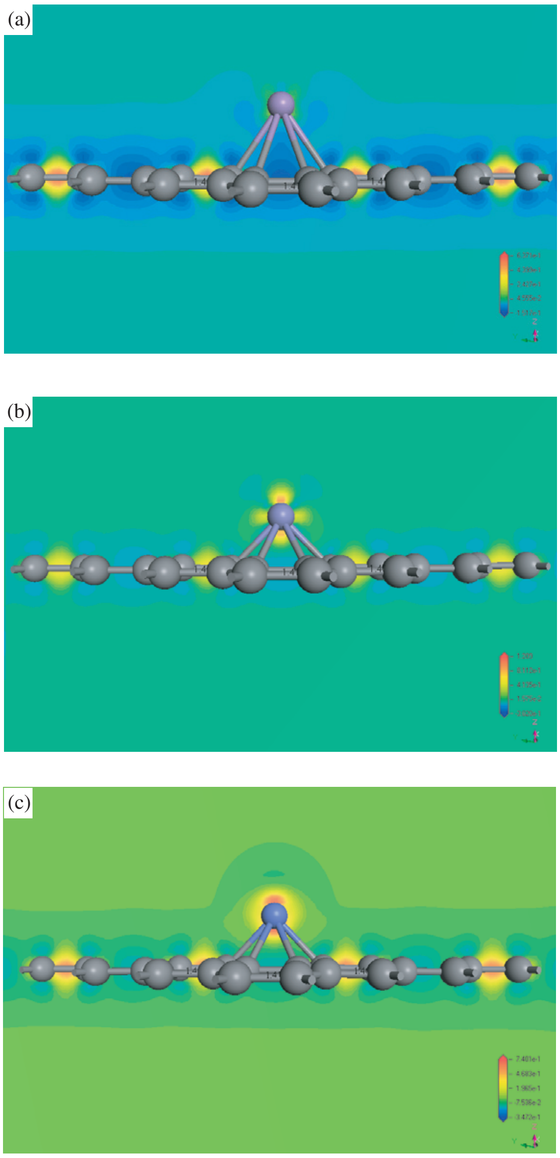

Figure 2. The optimized structures and the difference in charge density (eV $(\text{au})^{-3}$) for the most stable configurations of Mn (a), Fe (b), and Co (c). The difference in charge density is plotted in a slab which is perpendicular to the graphene layer (xy plane) and contains the adatom.

graphene, the DFT calculations performed here are for the graphite surface with large vacuum seperations. Graphene–substrate interaction needs to be considered when applying our results to the substrate-based graphene systems.

Before relaxation, a series of static calculations are performed to determine the interaction potential of adatoms with graphene. In this process, the adatoms are kept fixed at different distances along a line perpendicular to the graphene layer. For each adatom, we optimize the geometry at each global minimum of total energy curves and then compare the total energy to determine the proper adatom–graphene distance. The relative stabilities of different adatom–graphene systems are determined by the adsorption energies. For instance, larger absolute values of the adsorption energy mean strong binding of the adatom to the surface of graphene. The adsorption energy is defined by the formula

$$E_{\text{adsorption}} = E_{(\text{adatom+graphene})} - E_{\text{graphene}} - E_{\text{adatom}}, \qquad (1)$$

where $E_{(\text{adatom+graphene})}$ is the spin-polarized total energy for the optimized equilibrium configuration of the graphene and the adatom, E_{graphene} is the total energy of the isolated graphene, and E_{adatom} is the spin-polarized total energy of the corresponding adsorption adatom in its ground state. A summary of the results for the optimized structures is given in table 1. In table 1, we find that the H site is the most stable for Mn, Fe, Co after optimization. The reason for the H site being the most optimal one is that it has the largest number of neighboring C atoms for lowering the adsorption energy. Our re-relaxed calculations on the three kinds of TM adatoms in H sites show that the adatoms that break the symmetry will return to the H position. The fact that some of the adsorption sites, for example B and T sites, are found to be unstable also suggests that symmetry-lowering distortions are not suitable for adatoms to stay. Our stable sites for Mn, Fe and Co are in agreement with those found by Yosuke Yagi *et al* [12]. Table 1 shows that the adatom–C distance (bond length) at the most stable site differs with the variation of adatoms. The Mn–C bond length of 2.52 Å is the longest. The bond lengths of 2.08 Å for Fe and 2.09 Å for Co are very close to the values (2.12 Å for Fe and 2.10 Å for Co) obtained by Yosuke Yagi *et al* [12]. The heights of 1.47 Å for adatom Fe and 1.56 Å for Co on graphene surface are also highly consistent with the result in [12].

Figures 2(a)–(c) show the optimized stable configurations and their corresponding difference in charge density for the Mn, Fe and Co adatom systems. The difference in charge density is obtained by subtracting the electron density of the separated adatom and graphene from the density of the whole system. In figure 2, the difference in charge density is plotted in

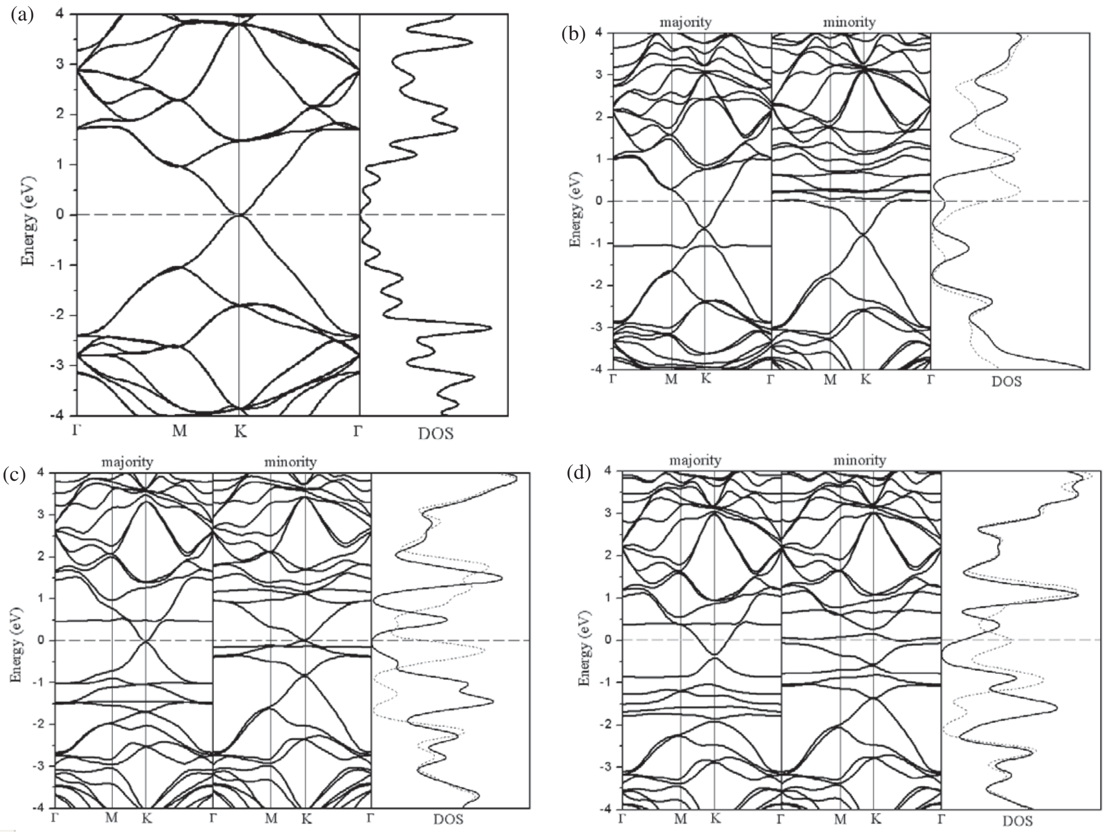

Figure 3. (a) The band structure and corresponding DOS of pure graphene in the 4 × 4 supercell. The majority and minority band structures and corresponding DOS of the adatom–graphene systems at the most stable configurations are shown, (b) for Mn, (c) for Fe and (d) for Co. Solid and dotted lines in the DOS are for majority and minority spin states, respectively. The Fermi level is indicated by the dashed line.

a slab that is perpendicular to the graphene layer (xy plane) and contains the adatom. As suggested by Khantha *et al* [10], the redistribution of charge density indicates that the interaction potential between the adatom and graphene is composed of two distinct contributions: a screened Coulomb interaction resulting from the charge transfer between the adatom and C atoms, and a van der Waals type interaction. It is well known that the DFT approach does not describe the van der Waals interactions correctly at large separations [26]. However, the adatom–graphene system studied here is not a pure van der Waals system due to the charge redistribution at short adatom–graphene separations. The equilibrium position of an adatom above graphene is largely determined by the charge redistribution that takes place in this short-separation region. The charge redistribution in the region of the hexagonal carbon ring surrounding Mn, Fe and Co (figures 2(a)–(c)) is different in appearance and magnitude when compared with isolated atoms of Mn, Fe and Co. From table 1, we can find that there are 0.84e, 1.28e and 1.10e charges being transferred for Mn, Fe, and Co. These factors lead to enhanced bonding at these positions for Mn, Fe and Co, and consequently larger adsorption energy in absolute value when compared to other configurations. The adsorption energies for the most stable configuration of Mn, Fe, and Co are −0.93, −1.42, and −1.32 eV, respectively. An important aspect of adatom absorption on graphene is the magnetic behavior of the adatom. It is well known that the 3d TM atoms Mn, Fe and Co possess magnetic moments of 5, 4 and 3 μ_B, respectively [27]. When supported on graphene, the magnetic moment for an Mn atom is enhanced by 0.56 μ_B, while those of Fe and Co atoms are reduced by about 2 μ_B from their free atom states. The high magnetic moment of Mn on graphene may be useful for spin electronic devices.

Figures 3(b)–(d) show the spin-polarized band structures and corresponding density of states (DOS) of the adatom–graphene systems with Mn, Fe and Co as adatoms, respectively. For comparison, the band structure of pure graphene is plotted in figure 3(a). Our result shows that pure graphene is a zero-gap semiconductor or a semi-metal, which is consistent with the conclusion in the literature [4, 28]. By Mn adatom adsorption (figure 3(b)), we can find that a flat band appears just under the Fermi level (In CASTEP, the Fermi level is set to the band center and all energies are relative to the Fermi level) in majority spin bands, which corresponds to the Mn 4s orbital, as can be derived from the local density of states (LDOS) (figure 4(a)). In the case of minority spin, the Mn atom introduces localized states with d orbital character near the Fermi level in the conduction band, which can also be concluded from the minority d orbital in the LDOS of Mn, as shown in figure 4(a). The conduction bands are modified and move down due to the coupling between the Mn atom and graphene both in majority-spin and minority-spin bands. There

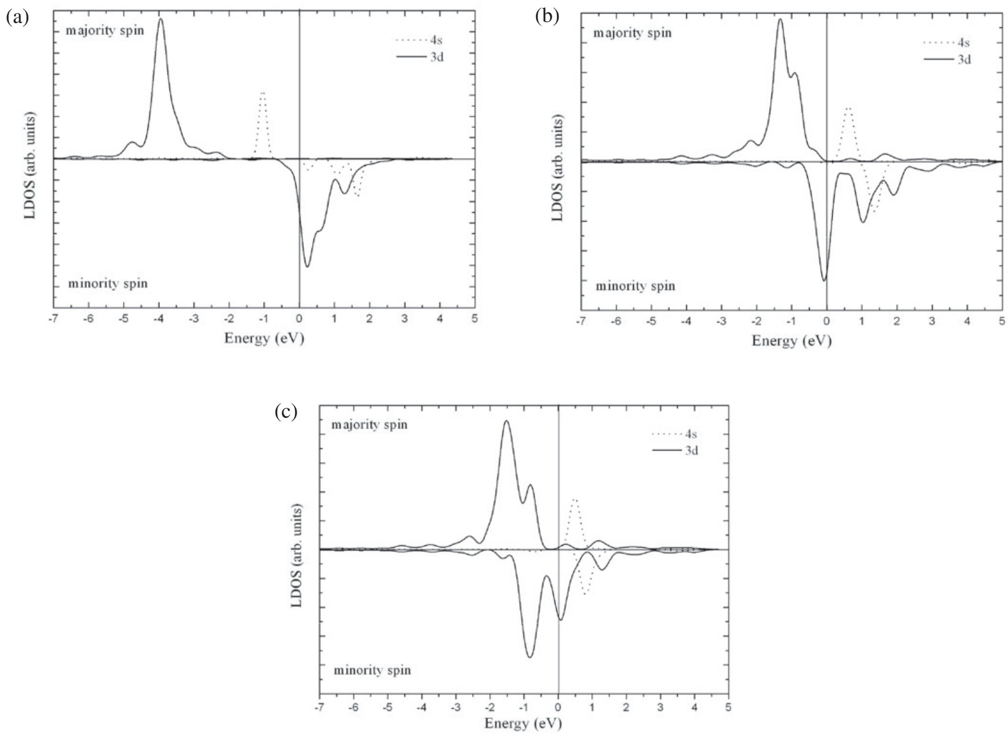

Figure 4. Local density of states (LDOS) of Mn (a), Fe (b) and Co (c) adatoms in the stable configurations on graphene. The Fermi level is indicated by the solid line at $E = 0$.

is complete polarization at the Fermi level and the system exhibits metallic character; in other words, half-metallicity does not occur. The energy band analysis indicates that Fe (figure 3(c)) adsorbed on the graphene surface is semi-half-metallic, namely the system is metallic for minority spin, but two bands with p_z character cross precisely at the k point in majority spin at the Fermi level and keep the zero value in the plot of the DOS. Spin polarization $P(E_F)$, based on the definition [29] of

$$P(E_F) = [D(E_{F,\uparrow}) - D(E_{F,\downarrow})]/[D(E_{F,\uparrow}) + D(E_{F,\downarrow})], \quad (2)$$

where $D(E_{F,\uparrow})$ and $D(E_{F,\downarrow})$ represent the DOS of majority and minority spin at the Fermi level, is found to be 100%. As most transport occurs around the Fermi level, this high spin polarization ensures a high degree of passage of the preferred spin. In carbon nanotubes, Yang *et al* [30] found that a chromium or vanadium atomic chain adsorbed on an armchair carbon nanotube opened up a band gap for the minority spin, also making the whole system a 100% spin-polarized conductor, and the adsorption of manganese, iron, cobalt, or nickel chains leads to large but incomplete spin polarization. In figure 3(d), the π band is shifted down by ~ -0.5 eV in majority spin and ~ -1.5 eV in minority spin, respectively. In this case, the d orbitals of Co strongly hybridize with the carbon p_z orbitals. In figures 3(c) and (d), the flat bands from the 4s orbital of Fe and Co adatoms all appear above the Fermi level in majority spin, which is different from that of an Mn adatom on graphene. The combined system of an Co adatom on graphene exhibits metallic electronic structure due to the DOS peak at the Fermi level. Our results for the adatom–graphene system suggest a feasible new method for achieving the goal of perfect spin polarization and also provide a useful tool for band gap engineering on the single atomic carbon layer.

To have a better understanding of the magnetism of adatom adsorption on graphene, in figure 4 we illustrate the LDOS on the adatoms. In the case of the adsorption of Mn on graphene (figure 4(a)), although the minority-spin s character levels for Mn are also unoccupied, the corresponding majority-spin levels are above the Fermi level and are occupied. From figure 4(b), we can see that the s states of Fe lie predominantly above the Fermi level and are thus unoccupied. This result is similar to the observations of Fe atoms adsorbed on the external surfaces of a (8, 0) single-walled carbon nanotube (SWCNT) [31] and of a (4, 4) SWCNT [32]. From figure 4(c) for Co, one can also find that the 4s states do not show a significant contribution to the occupied states, since almost all the 4s weight is located above the Fermi energy. Thus, we observe a larger promotion of the 4s electrons into the 3d states in figures 4(b) and (c) compared with that for Mn in figure 4(a), resulting in lower local moments for Fe and Co than for Mn on graphene.

In conclusion, we have studied the stable geometries and spin electronic structures of Mn, Fe and Co adsorbed on graphene (a single graphite layer) using the first-principle plane-wave method. We find that the H site is the most stable for Mn, Fe, Co after optimization. The calculated spin-polarized band structures of the graphene encapsulating the Mn adatom indicate that the conduction bands are modified and move down due to the coupling between the Mn atom and graphene. The energy band analysis indicates that Fe adsorbed on the graphene surface is semi-half-metallic, and spin polarization $P(E_F)$ is found to be 100%. The hybrid structures can therefore be applied to circuits that demand the preferential transport of electrons with a specific spin. The combined system of a Co adatom on graphene exhibits metallic electronic structure due to the DOS peak at the Fermi level both with majority spin and minority spin. The LDOSs indicate a larger promotion of the 4s electrons into the 3d states in Fe and Co, resulting in lower local moments compared to an Mn adatom on the graphene surface. The control of spin-polarized band structures and magnetic properties in adatom–graphene systems may find potential applications in the realization of graphene-based electronic and spintronic devices.

Acknowledgments

This work was supported by the National Natural Science Foundation of China (grant no. 10774127), by the Research Foundation of Hunan Provincial Education Department (grant nos 05A005 and 07C748), by the Across Subject Program of Xiangtan University (grant no. 06IND02), and by the Chang Jiang Scholars Program, Ministry of Education, China.

References

[1] Novoselov K S, Geim A K, Morozov S V, Jiang D, Zhang Y, Dubonos S V, Grigorieva I V and Firsov A A 2004 *Science* **306** 666

[2] Berger C, Song Z, Li T, Li X, Ogbazghi A Y, Feng R, Dai Z, Marchenkov A N, Conrad E H, First P N and de Heer W A 2004 *J. Phys. Chem.* B **108** 19912

[3] Schniepp H C, Li J L, McAllister M J, Sai H, Herrera-Alonso M, Adamson D H, Prud'homme R K, Car R, Saville D A and Aksay I A 2006 *J. Phys. Chem.* B **110** 8535

[4] Saito R, Dresselhaus G and Dresselhaus M S 1998 *Physical Properties of Carbon Nanotubes* (London: Imperial College Press)

[5] Novoselov K S, Geim A K, Morozov S V, Jiang D, Katsnelson M I, Grigorieva I V, Dubonos S V and Firsov A A 2005 *Nature* **438** 197

[6] Zhang Y, Tan Y-W, Stormer H L and Kim P 2005 *Nature* **438** 201

[7] González J and Perfetto E 2007 *Phys. Rev.* B **76** 155404

[8] Cheianov V V, Fal'ko V and Altshuler B L 2007 *Preprint* cond-mat/0703410 v1

[9] McCann E and Fal'ko V I 2006 *Phys. Rev. Lett.* **96** 086805

[10] Khantha M, Cordero N A, Molina L M, Alonso J A and Girifalco L A 2004 *Phys. Rev.* B **70** 125422

[11] Duffy D M and Blackman J A 1998 *Phys. Rev.* B **58** 7443

[12] Yagi Y, Briere T M, Marcel Sluiter H F, Kumar V, Farajian A A and Kawazoe Y 2004 *Phys. Rev.* B **69** 075414

[13] Duffy D M and Blackman J A 1998 *Surf. Sci.* **415** L1016

[14] Duplock E J, Scheffler M and Lindan P J D 2004 *Phys. Rev. Lett.* **92** 225502

[15] Lehtinen P O, Foster A S, Ayuela A, Krasheninnikov A, Nordlund K and Nieminen R M 2003 *Phys. Rev. Lett.* **91** 017202

[16] Hao S G, Zhou G, Duan W H, Wu J and Gu B L 2006 *J. Am. Chem. Soc.* **128** 8453

[17] Segall M D, Lindan P L D, Probert M J, Pickard C J, Hasnip P J, Clark S J and Payne M C 2002 *J. Phys.: Condens. Matter* **14** 2717

[18] Lehtinen P O, Foster A S, Ayuela A, Krasheninnikov A, Nordlund K and Nieminen R M 2003 *Phys. Rev. Lett.* **91** 017202

[19] Mao Y L, Yan X H and Xiao Y 2005 *Nanotechnology* **16** 3092

[20] Mao Y L, Zhong J X, Yuan J M, Zhao X L and Ando Y 2006 *J. Nanosci. Nanotechnol.* **6** 1482

[21] Mao Y L, Yan X H, Xiao Y, Xiang J and Yang Y R 2005 *Phys. Rev.* B **71** 033404

[22] Mao Y L, Yan X H, Xiao Y, Xiang J, Yang Y R and Yu H L 2004 *Nanotechnology* **15** 1000

[23] Perdew J P, Burke K and Ernzerhof M 1996 *Phys. Rev. Lett.* **77** 3865

[24] Vanderbilt D 1990 *Phys. Rev.* B **41** 7892

[25] Monkhorst H J and Pack J D 1976 *Phys. Rev.* B **13** 5188

[26] Andersson Y, Langreth D and Lundqvist B I 1996 *Phys. Rev. Lett.* **76** 102

[27] Ma L, Zhao J, Wang J, Wang B and Wang G 2007 *Phys. Rev.* B **75** 045312

[28] Perdew J P and Wang Y 1992 *Phys. Rev.* B **45** 13244

[29] Durgun E and Ciraci S 2006 *Phys. Rev.* B **74** 125404

[30] Yang C, Zhao J and Lu J P 2004 *Nano Lett.* **4** 561

[31] Fagan S B, Mota R, da Silva A J R and Fazzio A 2003 *Phys. Rev.* B **67** 205414

[32] Andriotis A N, Menon M and Froudakis G 2000 *Phys. Rev. Lett.* **85** 3193